

# Online Health-Conscious Energy Management Strategy for a Hybrid Multi-Stack Fuel Cell Vehicle Based on Game Theory

Razieh Ghaderi, *Member, IEEE*, Mohsen Kandidayeni, *Member, IEEE*, Mehdi Soleymani, *Member, IEEE*, Loïc Boulon, *Senior Member, IEEE*, João P. Trovão, *Senior Member, IEEE*

**Abstract**—The use of multiple low-power fuel cells (FCs), instead of a high-power one, in the powertrain of a FC-hybrid electric vehicle (FC-HEV) has recently received considerable attention. This is mainly due to the fact that this configuration can lead to higher efficiency, durability, and reliability. However, the added degrees of freedom require an advanced multi-agent energy management strategy (EMS) for an effective power distribution among power sources. This paper puts forward an EMS based on game theory (GT) for a multi-stack FC-HEV with three FCs and a battery pack. GT is a well-approved method for characterizing the interactions in multi-agent systems. Unlike the other strategies, the proposed EMS is equipped with an online identification system to constantly update the time-varying characteristics of the power sources. The performance of the suggested strategy is investigated through two case studies. Firstly, a comparative study with two other EMSs, dynamic programming (offline), and a competent rule-based strategy (online), is conducted to realize the capability of GT. Secondly, to justify the necessity of online system identification, the degradation effect of each power source on the EMS performance is examined. The carried-out studies show that the total cost (hydrogen consumption and degradation) of the proposed strategy is almost 6% better than the rule-based EMS while keeping a reasonable difference with dynamic programming. Moreover, health unawareness of power sources can increase the hydrogen consumption up to 7% in the studied system.

**Index Terms**—Fuel cell and battery degradation, game theory, multi-stack fuel cell hybrid electric vehicle, modular system, online energy management strategy.

## I. INTRODUCTION

A FC-HEV is often composed of a proton exchange membrane (PEM) FC and a battery pack. As the energetic char-

This research was funded by Natural Sciences and Engineering Research Council of Canada (NSERC) [RGPIN-2018-06527 and RGPIN-2017-05924], Canada Research Chairs program [950-230863 and 950-230672], and Fonds de Recherche en Santé Québec-Nature et technologies (FRQNT) [Bourses de recherche postdoctorale B3X, file number: 284914].

R. Ghaderi and L. Boulon are with the Hydrogen Research Institute, Department of Electrical and Computer Engineering, Université du Québec à Trois-Rivières, QC G8Z 4M3, Canada (email: Razieh.Ghaderi@uqtr.ca, Loic.Boulon@uqtr.ca).

M. Kandidayeni is with Department of Electrical Engineering and Computer, Université de Sherbrooke, Sherbrooke, QC, J1K 2R1, Canada, and also with the Hydrogen Research Institute, Université du Québec à Trois-Rivières, QC G8Z4M3, Canada (e-mail: Mohsen.Kandidayeni@USherbrooke.ca).

M. Soleymani is with department of Mechatronics Engineering, Arak University, Arak, Iran (email: m-soleymani@araku.ac.ir).

J. P. F. Trovão is with the Department of Electrical Engineering and Computer Engineering, Université de Sherbrooke, Sherbrooke, QC, J1K 2R1, Canada, and also with Polytechnic of Coimbra (IPC-ISEC) and INESC Coimbra, Portugal (e-mail: Joao.Trovao@USherbrooke.ca).

acteristics of the utilized sources in a FC-HEV are different, the use of an energy management strategy (EMS) is essential to minimize the hydrogen consumption and maximize the lifetime of the system [1]. Several EMSs, namely rule-based and optimization-based have been proposed for a FC-HEV with a single-stack configuration. The rule-based strategies are typically heuristic and lead to sub-optimal results unless being well tuned. Therefore, the use of optimization techniques has come under attention which are also capable of improving the rule-based strategies. Optimization-based category falls into two groups of global, such as dynamic programming (DP) [2], and real-time, like equivalent consumption minimization strategy (ECMS) [3] and Pontryagin's minimum principle (PMP) [4], strategies considering the specified cost function. In [5], a two-stage strategy is designed for a FC-HEV where a predictive controller is used to determine the global battery state of charge (SOC) trend as well as the local control references. In [6], a supervisory control scheme based on optimized fuzzy logic is proposed to distribute the power between a FC stack and supercapacitor (SC) under different driving cycles. In [7], an EMS based on model predictive control (MPC) is proposed for a FC-HEV, considering FC, battery, SC, hydrogen, and charge sustaining costs. In [8], a rule-based strategy is proposed for the same FC-HEV while all the operational costs are controlled by imposing constraints to the sources. In [9], a rule-based EMS is developed for dual-locomotive. This work has proposed an always-on strategy to prevent the on/off cycling in the FC system. In [10], multidimensional DP is developed for a FC-HEV. This paper introduces a sign function to reduce the number of on/off cycling in the FC system. However, FC-HEVs with a single-stack structure are susceptible to the malfunction of the power sources and limited in terms of efficiency. Hence, it is essential to improve them in terms of efficiency, durability, and cost. One of the feasible options in this regard is the development of a hybrid multi-stack FC system which is composed of multiple connected low-power FCs rather than a high-power one along with an energy storage system.

Various configurations for a multi-stack FC system are studied in [11] and is shown that a parallel structure, where each FC is connected to the bus through a DC-DC converter, can provide better efficiency and enhance the reliability due to the inherent redundancy. Some of the key advantages of a parallel multi-stack powertrain configuration are as follows:

- Efficiency and durability enhancement: a single-stack FC

system has solely one optimal operating point while a multi-stack system provides access to several ones. This feature provides a wider high-efficiency operation zone and more degrees of freedom for power distribution which also leads to increase of FCs lifetime.

- High survivability: survivability is increased by providing more redundancy in a multi-stack system. In fact, this configuration decreases the possibility of a complete operation halt as it enables degraded mode of operation in a FC-HEV.

- Flexible structure: this structure provides a flexible arrangement that is significant for mass distribution and stability of the vehicle. However, to benefit from the above-mentioned advantages that originate from the utilized hardware (parallel multi-stack configuration), an advanced EMS (as a software) is required.

In [12], four FCs are connected to the DC bus through DC-DC converters to reach higher output voltage while utilizing a maximum power (MP) point tracking tool for each stack. In [13], a hierarchical control method, composed of a control and a management layer, is proposed for a multiple FC system. The equivalent fitting circle method is used in this study to realize the optimal allocation among the FCs. In [14], an adaptive current sharing technique based on droop control is suggested for two FCs to decrease the degradation rate. In [15], a hysteresis EMS is designed for a multi-stack FC-HEV with three FCs and a battery pack. The objective of this strategy is to equalize the operational time of the three FCs while declining the number of on-off cycles. In [16], an EMS based on auxiliary problem principle is proposed for a multi-stack FC-HEV with two FCs and a battery pack. The results of this work demonstrate that this real-time approach is able to attain an end-user price very near to DP. All the above-discussed manuscripts have attempted to propose a new methodology to satisfy all the expectations from a multi-source system (minimizing the hydrogen consumption and enhancing the lifetime of each individual powertrain). However, this is a highly difficult task as each of the components have their own particular interests. One of the most practical techniques for dealing with a multi-objective problem in the presence of several agents (power sources herein) is game theory (GT). The performance of GT has been already justified for the energy management of single-stack FC-HEVs [17], [18].

However, its deployment in a multi-stack FC-HEV, which is a multi-agent system, has escaped the attention. GT can define a wide range of interactions between multiple power sources. Compared to the above-discussed papers, GT has a convenient framework for understanding the preference in situations among different agents and can help them reach optimal decision-making in various conditions.

Considering the discussed points, this paper proposes an online EMS based on GT for a multi-stack FC-HEV. The powertrain of this vehicle is composed of three FCs and a battery pack. The proposed strategy aims to maximize the self-interest of each individual power source while minimizing the hydrogen consumption of the system. To the best of the authors' knowledge, this is one of the first attempts, if any, to distribute the power/energy flow in a multi-stack FC-HEV using GT. According to the literature, one of the main causes

of mismanagement in any EMS is the performance drifts of the power sources owing to degradation and operating conditions variations [19]. To deal with this issue, each power source in this work is combined with an online parameter estimation tool using recursive least square (RLS) to track the health state of the components and extract the updated energetic characteristics. Combining the GT with online identification of power sources leads to the development of a health-aware GT, which is another distinguishing feature of this manuscript. Two case studies are considered to verify the performance of the proposed strategy. In the first case study, it is compared with DP, as an optimal strategy, and a real-time rule-based EMS under a real driving cycle. In the second case study, the effect of power sources' degradation over the performance of the EMS is considered to evaluate the robustness and necessity of the integrated online identification tool.

The rest of the paper is organized as follows. Section II describes the characteristic of the multi-stack FC-HEV. Section III explains the EMS development. The obtained results from three EMSs are discussed in section IV. Finally, the conclusion is given in section V.

## II. POWERTRAIN MODELING

Fig. 1 illustrates the configuration of the utilized multi-stack FC-HEV in this study, which belongs to a three-wheel electric vehicle from e-TESC laboratory of University of Sherbrooke [20]. According to this figure, three FCs and a small battery pack, that are all connected to the DC bus through individual DC-DC converters, are considered to supply the requested power of this vehicle. Table I shows the specifications of this vehicle.

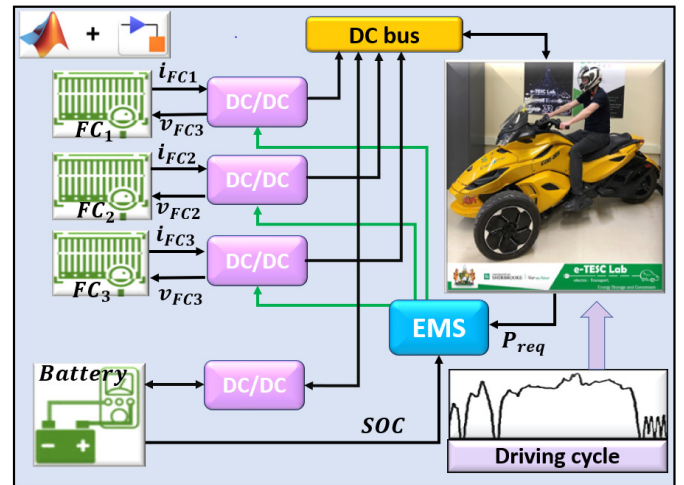


Fig. 1. The hybrid multi-stack powertrain configuration for the three-wheel electric vehicle at e-TESC lab., University of Sherbrooke.

The energetic macroscopic representation (EMR) of the traction system, which is used for the EMS development, is shown in Fig. 2. EMR is a recognized formalism for modeling FC-HEVs [21]. The related equations are as follows:

$$\frac{dV_{EV}}{dt} = \frac{F_{tr} - F_{env}}{m_{eq}} \quad (1)$$

TABLE I  
SPECIFICATION OF E-TESC THREE-WHEEL VEHICLE.

Variable	Symbol	Value	Unit
Vehicle mass	$M_{eq}$	350	kg
Typical rolling resistance coefficient	$\mu_{fr}$	0.02	-
Typical aerodynamic drag coefficient	$C_D$	0.75	-
Vehicle front area	$A_f$	1.25	m
Wheel radius	$r$	0.305	m <sup>2</sup>
Belt transmission drive ratio	$G_{gb}$	5.033 (30:151)	-

$$F_{tr} = \frac{G_{gb}}{r} T_{em} \eta_{gb}^{\beta} \quad (2)$$

$$F_{tr} = F_{roll} + F_{grade} + F_{air} \quad (3)$$

$$F_{roll} = M_{eq} g \mu_{fr} \cos \Theta \quad (4)$$

$$F_{air} = 0.5 \rho_{air} A_{aero} C_d V_{EV}^2 \quad (5)$$

$$F_{grade} = m_{eq} g \sin \Theta \quad (6)$$

$$\Omega_m = \left( \frac{G_{gb}}{r} \right) V_{EV} \quad (7)$$

$$i_{ts} = \frac{T_{em} \Omega_m \eta_m^{\beta}}{u_{DC}} \quad (8)$$

where  $F_{tr}$  is the traction force,  $F_{env}$  is the vehicle traction force resistance,  $M_{eq}$  is the equivalent of vehicle mass,  $r$  is the wheel radius,  $T_{em}$  is the electric machine torque,  $\eta_{gb}$  is the gearbox transmission efficiency,  $\rho_{air}$  is the air density (1.2 kg/m<sup>3</sup>),  $\beta$  is -1 or 1 depending on the braking mode,  $\Omega_m$  is the rotor rotation speed,  $\Theta$  is the road grade,  $\mu_{fr}$  is the rolling resistance,  $C_d$  is the aerodynamic drag,  $T_{em,ref}$  is the torque reference,  $u_{DC}$  is the voltage of DC bus, and  $\eta_m$  is the drive efficiency that considers the inverter and motor efficiency.

#### A. Fuel Cell model

In this study, a semi-empirical model proposed by Squadrito et al. is used to estimate the PEMFC output voltage [22]. This semi-empirical model can fit the experimental data over the whole range of current density with high accuracy. It has only four parameters to be tuned and requires two sensors (voltage, and current) to be adapted to a new FC system. These features have made this steady-state model very suitable for energy management application where its appropriateness has been already confirmed [23]. The required experimental data to tune the parameters of the model have been extracted from tests of a Ballard Power System (FCvelocity®-9SSL) designated for transportation applications. Fig. 3 shows the polarization behavior of the utilized FC from Ballard Power System.

According to this model, the output voltage is calculated by:

$$V_{FCi} = N[V_o - b \log(J) - R_{internal} J + \delta J^T \ln(1 - \beta J)] \quad (9)$$

where  $N$  is the number of cells,  $V_{st}$  is the output voltage (V) of the stack,  $V_o$  is the reversible cell potential (V),  $b$  is the Tafel slope,  $J$  is actual current density (cm<sup>2</sup> A<sup>-1</sup>),  $R_{internal}$  is cell resistance ( $\Omega$ ),  $\alpha$  is a semi-empirical parameter related to the diffusion mechanism,  $\sigma$  (between 1 and 4) is a dimensionless number which is related to the water flooding phenomenon,

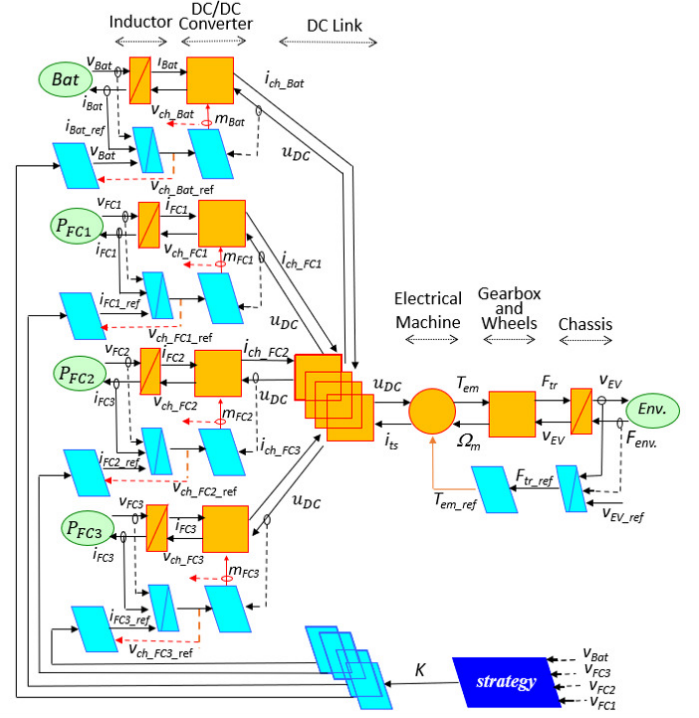


Fig. 2. The studied multi-Stack FC-HEV powertrain EMR.

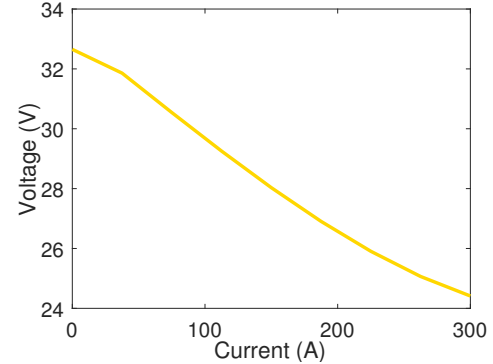


Fig. 3. Polarization curve of the utilized FC system.

and  $\beta$  is the inverse of the limiting current density (cm<sup>2</sup> A<sup>-1</sup>).  $V_o$ ,  $b$ ,  $R_{internal}$  and  $\alpha$  need to be identified by an online estimator to achieve an accurate voltage estimation. In order to verify the effect of FCs degradation on the EMS performance, a simple aging model is used to emulate the voltage decline of each FC under constant load and on-off cycling. The end-of-life (EOL) criterion according to US department of Energy for the FC is assumed as a 10-percent decline in the MP. The following equation describes the output voltage of the aging model.

$$V_{FC} = V_o \exp(\varsigma, t) - \Delta V k \quad (10)$$

Where  $\varsigma$  is a constant coefficient,  $V_o$  is the stack voltage of the new PEMFC,  $K$  is the number of on/off cycles,  $t$  is the operation time, and  $\Delta V$  is the FC voltage drop owing to one start-stop cycle. For the current FC,  $\Delta V$  is assumed 13.79  $\mu V/cycle$  [24]. The losses from the balance of plant

(compressor and fan) have been calculated based on the proposed formulations in [24]. Moreover, an experimental equation based on stack current ( $I_{st}$ ) and number of cells ( $N_{cell}$ ) is used to determine the hydrogen flow ( $q_{H_2}$ ) [25] as:

$$q_{H_2} = 0.00696 I_{st} N_{cell} \quad (11)$$

### B. Battery model

The battery pack comprises a series-parallel combination of Li-ion cells. The specifications of the Li-ion cell and FC are shown in Table II. The battery behavior is simulated by the Thevenin model, which is a dynamic type. It is composed of an ideal voltage source to characterize open circuit voltage (OCV) as a function of SOC, a series ohmic resistance, and a parallel RC branch. Depending on the required accuracy, the number of parallel RC branches can vary from 1 (known as Thevenin equivalent circuit model) to  $n$ . Thevenin models have been already utilized in energy management of FC-HEVs [26]. In this model, the OCV is obtained by:

$$V_{oc} = V_{bat} - (R_s + R_c)I_{bat} + R_c C_c \frac{dv_{bat}}{dt} - R_s R_c C_c \frac{dI_{bat}}{dt} \quad (12)$$

where  $V_{bat}$  is the terminal voltage,  $V_{oc}$  is the OCV,  $I_{bat}$  is the battery load current (positive and negative currents correspond to charge and discharge respectively),  $R_s$  is the internal ohmic resistance, and  $R_c$  and  $C_c$  are the equivalent polarization resistance and capacitance, respectively. To estimate a precise terminal voltage, the equivalent circuit model (ECM) parametrization should be done by an online parameter estimation technique. The prerequisite laboratory test data for the identification process has been provided by performing charge and discharge pulse testes. In order to estimate the SOC, coulomb counting formula is used. To see the impact of battery degradation on the performance of the multi-stack FC-HEV, the common battery ageing criteria are utilized in which the internal resistance is doubled, or the capacity is faded by 20 percent [19]. As a result, the SOC calculations are updated according to the state of the health of the battery.

TABLE II  
THE CHARACTERISTICS OF POWER SOURCES

Power Sources	Parameter	Symbol	Value	Unit
FC	No. cell	$N_{cell}$	38	cell
	No. stack	$N_{stack}$	3	-
	Max Current	$i_{FC,max}$	300	A
	Max Power	$P_{FC,max}$	7.33	kW
	Max Temperature	$T_{FC,max}$	70	°C
Battery	No. Series	$N_{bat,serie}$	24	-
	No. Parallel	$N_{bat,parallel}$	12	-
	Capacity	$Q_{bat}$	2.5	Ah
	Nominal Voltage	$V_{bat,nom}$	3.7	V

### C. Online parameter estimation

To counteract the influence of the characteristics variation uncertainties, RLS, as an attested estimator in the literature, has been utilized for the parameters' adjustment of both power sources. The details about adopting RLS for estimating the

parameters of the above-explained battery and PEMFC models are available in [27], [28]. Consequently, only the obtained results from the online parameters identification are discussed in this section. Fig. 4(a) presents the estimation of the PEMFC output voltage performed via RLS. According to the reported mean square error (MSE) in the caption of this figure, the tuned model can imitate the behavior of the real FC with a good accuracy. Fig. 4(b) also represents the estimation of the FC power curve which is close to the measured one. Fig. 5(a) shows a pulse charge test applied to the Li-ion cell to perform the model parametrization. The parameters of the ECM model are identified using RLS. Fig. 5(b) illustrates the estimation of the terminal voltage. Figs. 5(c) and 5(d) give an account of the estimation of the equivalent resistor and open circuit voltage, respectively. The estimation of the battery parameters confirms the accuracy of the performed identification.

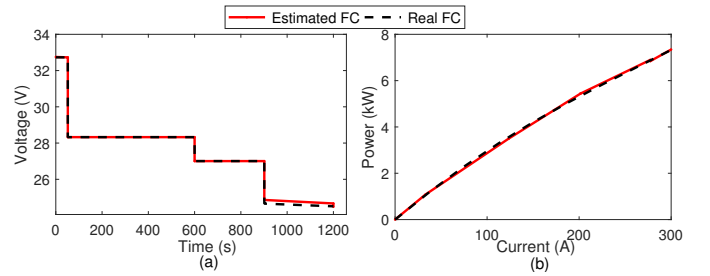


Fig. 4. The estimated voltage and power curves: MSE (a):0.01, MSE (b):0.003.

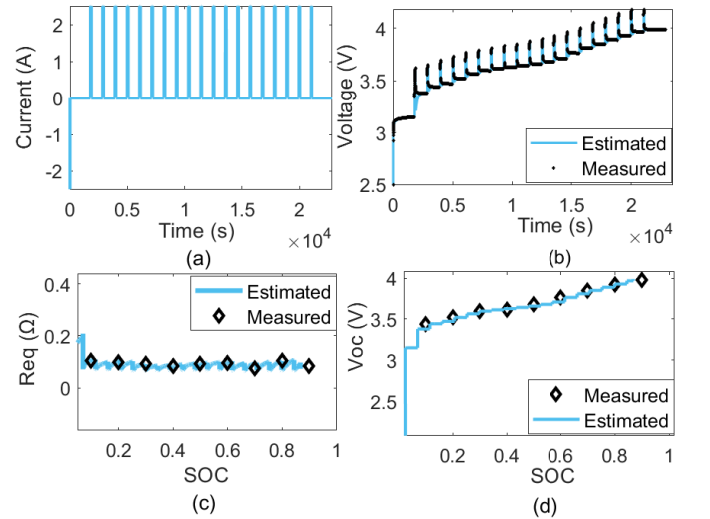


Fig. 5. Battery Parameters in charge profile: (a) Current in charge profile, (b) The estimated terminal voltage, (c) Equivalent resistor, (d) Open circuit voltage.

## III. ENERGY MANAGEMENT STRATEGY

Battery and FCs are used to supply the requested power ( $P_{req}$ ) from the electric motor. Consequently, the hydrogen consumption of a multi-stack FC-HEV depends to a great extent on the distribution of the power between the PEMFCs and the battery. The aim of using an EMS is to determine a power

split trajectory to minimize the hydrogen consumption and maximize the lifetime of the power sources while respecting the limitations of the system.

$$P_{req} = \eta_{DC-DC}(P_{FC1} + P_{FC2} + P_{FC3} + P_{Bat}) \quad (13)$$

where  $P_{req}$  is the requested power,  $\eta_{DC-DC}$  (0.96) [29] is the DC-DC converter efficiency and  $P_{Bat}$  is the battery power. Hereinafter, GT (as the proposed EMS), DP (as an offline optimal reference), and ASM (as a real-time benchmark strategy) are explained.

### A. Game Theory

To reach a fair trade-off among the various individual preferences, it is vital to benefit from the attributes of each component and also the cooperation among them. GT is a well-approved method for characterizing the interactions among self-regarded players (power sources herein) and predicting their policies. Nash equilibrium is the most common method for noncooperative games including two or more players. A Nash equilibrium is reached when each power source has picked a policy and no other source can gain benefits by changing policies separately while the others keep their policies unchanged. Fig. 6 shows the developed multi-agent EMS in which three FCs and a battery pack are considered as four players interacting with the environment (i.e., the requested power here). According to Fig. 6, the online identification process is run for each of the FC systems and the battery pack while the vehicle is under operation. The responsibility of this identification process is to provide the actual battery SOC level as well as the maximum power ( $P_{FC-max,i}$ ) and the power with maximum efficiency ( $P_{FC-opt,i}$ ) of each FC, where  $i = 1, 2, 3$ . These updated characteristics of the power sources will be used by the developed EMS based on GT for the distribution of the power. The preferences of the players (FC and battery pack) are defined by means of some utility functions that illustrate the satisfaction level of a player considering the interaction between its physical model and the requested power. The principal goal of the developed GT-based strategy is to perform the power distribution in a way to reach a balance among the preferences of the players.

For any reason, if one of the FCs degrades more than the others, their operational characteristics, such as MP and efficiency points, will be updated by the developed online identification systems and their operations will be restricted within the updated ranges. This implies that the FCs with higher MP values will provide more power than the degraded ones. The following utility functions in quadratic forms are considered for the power sources to ensure the existence of the Nash equilibrium and its uniqueness. A weighted sum utility function, composed of three objectives/preferences, is defined for managing the operation of the battery pack. The main preference of the battery pack is to protect itself to extend its own lifespan. To do so, attention to the amplitude and variation rate of the battery power as well as the battery SOC operation range is required. Regarding the operation of the FCs, three objectives, namely reduction of the power variation, efficient operation, and minimizing the number of on/off cycles, are

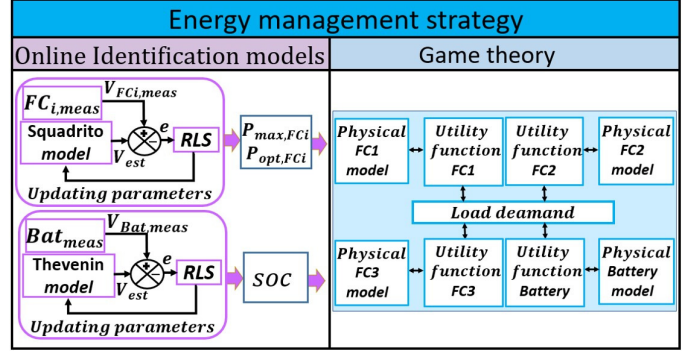


Fig. 6. The general scheme of the proposed GT based EMS for a multi-stack FC-HEV.

considered for each FC in this study. These three objectives are combined through the weighted sum method to form the utility function of each FC. Table III shows the list of utilized parameters for deriving the utility functions of the power sources in this work.

TABLE III  
INTRODUCING THE UTILIZED PARAMETERS FOR DEFINING THE UTILITY FUNCTIONS

Parameter	Symbol	Value
Maximum battery power	$P_{Bat,max}$	36.6 kW
Power variation rate	$P_{Bat,l}$	Previous battery power
Power amplitude rate	$P_{Bat,avg}$	Average battery power so far
Power variation rate	$P_{FC-l,i}$	Previous FC power
Power of maximum efficiency	$P_{FC-opt,i}$	Determined by the RLS algorithm
SOC variation rate	$SOC_l$	Previous SOC

The utility function of the battery ( $u_{Bat}$ ) is defined as:

$$u_{Bat} = u_{Bat,avg} + u_{Bat,soc} + u_{Bat,l} \quad (14)$$

where the function for limiting the battery power amplitude ( $u_{Bat,ave}$ ) is given by:

$$u_{Bat,avg} = w_{Bat,avg}(1 - f(P_{Bat} - P_{Bat,avg})^2) \quad (15)$$

The coefficient  $f$  is defined as below to normalize the value of  $u_{Bat,ave}$  between zero and one.

$$f = \text{Min}\left[\frac{1}{(P_{Bat,max} - P_{Bat,avg})^2}, \frac{1}{(-P_{Bat,max} - P_{Bat,avg})^2}\right]$$

The function for managing the battery SOC ( $u_{Bat,soc}$ ) is formulated as below which expresses the closeness to the desired initial SOC.

$$u_{Bat,soc} = w_{soc}(1 - g(-SOC_0 - SOC_l)^2) \quad (16)$$

The coefficient  $g$  is the normalizing factor to bring the value of  $u_{Bat,soc}$  within zero and one.

$$g = \text{Min}\left[\frac{1}{(P_{Bat,max} - P_{Bat,soc})^2}, \frac{1}{(-P_{Bat,max} - P_{Bat,soc})^2}\right]$$

The function for limiting the battery power variation  $u_{Bat,l}$  is defined as:

$$u_{Bat,l} = w_{Bat,l}(1 - c(P_{Bat} - P_{Bat,l})^2) \quad (17)$$

The normalizing factor  $c$  of  $u_{Bat,l}$  is given by:

$$c = Min\left[\frac{1}{(P_{Bat,max} - P_{Bat,l})^2}, \frac{1}{(-P_{Bat,max} - P_{Bat,l})^2}\right]$$

The weighted sum utility function for each FC is formulated as:

$$u_{FCi} = u_{FC_{opt},i} + u_{FC_{l},i} + u_{FC_{sgn},i} \quad (i = 1, 2, 3) \quad (18)$$

where  $i$  is the index for determining the FC number. The preference function for maintaining the FC operation in the efficient zone is obtained by:

$$u_{FC_{opt},i} = w_{opt,i}(1 - a_i(P_{FCi} - P_{FC_{opt},i})^2) \quad (i = 1, 2, 3) \quad (19)$$

The normalizing factor  $a$  is expressed as:

$$a_i = Min\left[\frac{1}{(P_{FC_{max},i} - P_{FC_{opt},i})^2}, \frac{1}{(P_{FC_{min},i} - P_{FC_{opt},i})^2}\right] \quad (i = 1, 2, 3)$$

The function for restricting the dynamic variation of each FC as well as their normalizing factor are given by:

$$u_{FC_{l},i} = w_{l,i}(1 - d_i(P_{FCi} - P_{FC_{l},i})^2) \quad (20)$$

$$d_i = Min\left[\frac{1}{(P_{FC_{max},i} - P_{FC_{l},i})^2}, \frac{1}{(P_{FC_{min},i} - P_{FC_{l},i})^2}\right] \quad (i = 1, 2, 3)$$

where  $P_{FC_{l},i}$  is the previous FC power and  $P_{FC_{max},i}$  is the MP of FC. To reduce the number of on/off cycles in the PEMFC, the following utility function  $u_{FC_{sgn},i}$  is utilized. This utility function has been introduced in [10] for controlling the on/off cycles in an offline EMS based on DP.

$$u_{FC_{sgn},i} = w_{sgn,i}(1 - sign(P_{FCi})^2) \quad (21) \quad (i = 1, 2, 3)$$

To comprehend the applicability of this function, let us assume that the FC stack is under operation (so it is on). As long as the FC keeps working, the value of this function is zero and has no effect on the total cost function. However, if the FC turns off and on, the sign function adds some costs to the total cost function. Therefore, in the performed optimization, the algorithm tries not to change the state of the FC a lot. If it is on, it attempts to keep it in this state as long as possible. If it is off, it prefers not to turn it on till necessary (the load condition in (13)). In this way, the proposed function prevents the frequent occurrence of on/off cycles in the FC systems. The FC stack power is between zero to 7330 W and therefore, its  $sign$  value is either zero or 1. It is worth noting that the same utility function has been used for other FC stacks as well. Finally, with the combination of utility functions of the battery and the FC the power that maximizes each utility function can be determined by applying the following derivations:

$$\frac{\partial u_{FCi}}{\partial P_{FCi}} = 0, \quad \frac{\partial u_{Bat}}{\partial P_{Bat}} = 0 \quad (i = 1, 2, 3) \quad (22)$$

The obtained best preferences can be written as:

$$\begin{aligned} S1 = & w_{opt,2} * a_2(P_{req} - P_{FC3} - P_{Bat} - P_{FC_{opt},1}) + \\ & w_{l,2} * d_2(P_{req} - P_{FC3} - P_{Bat} - P_{FC_{l},1}) + \\ & w_{sgn,2}(P_{req} - P_{FC3} - P_{Bat} - P_{FC_{sgn},1}) + \\ & w_{opt,3} * a_3(P_{req} - P_{FC2} - P_{Bat} - P_{FC_{opt},2}) + \\ & w_{l,3} * d_3(P_{req} - P_{FC2} - P_{Bat} - P_{FC_{l},2}) + \\ & w_{sgn,3}(P_{req} - P_{FC2} - P_{Bat} - P_{FC_{opt},1}) + \\ & w_{Bat,avg} * f(P_{req} - P_{FC2} - P_{FC3} - P_{FC_{opt},3}) + \\ & w_{Bat,l} * c(P_{req} - P_{FC2} - P_{FC3} - P_{FC_{l},3}) + \\ & w_{soc} * g(P_{req} - P_{FC2} - P_{FC3} - P_{FC_{sgn},3}) \end{aligned}$$

$$\begin{aligned} S2 = & w_{opt,1} * a_1(P_{req} - P_{FC2} - P_{FC3} - P_{FC_{opt},1}) + \\ & w_{l,1} * d_1(P_{req} - P_{FC2} - P_{FC3} - P_{FC_{l},1}) + \\ & w_{sgn,1}(P_{req} - P_{FC2} - P_{FC3} - P_{FC_{sgn},1}) + \\ & w_{opt,2} * a_2(P_{req} - P_{FC1} - P_{FC3} - P_{FC_{opt},2}) + \\ & w_{l,2} * d_2(P_{req} - P_{FC1} - P_{FC3} - P_{FC_{l},2}) + \\ & w_{sgn,2}(P_{req} - P_{FC2} - P_{FC3} - P_{FC_{sgn},2}) + \\ & w_{opt,3} * a_3(P_{req} - P_{FC1} - P_{FC2} - P_{FC_{opt},3}) + \\ & w_{l,3} * d_3(P_{req} - P_{FC1} - P_{FC2} - P_{FC_{l},3}) + \\ & w_{sgn,3}(P_{req} - P_{FC1} - P_{FC2} - P_{FC_{sgn},3}) \end{aligned}$$

$$\begin{aligned} G = & w_{opt,1} * a_1 + w_{opt,2} * a_2 + w_{opt,3} * a_3 + w_{l,1} * d_1 + \\ & w_{l,2} * d_2 + w_{l,3} * d_3 + w_{sgn,1} + w_{sgn,2} + w_{sgn,3} + \\ & w_{Bat,avg} * f + w_{Bat,l} * c + w_{soc} * g \end{aligned}$$

where  $P_{Bat}$  can be replaced by  $P_{FCi}$  using the power balance in (13). As it is seen in (23) and (24), there are twelve weight coefficients inside the derived equations. These coefficients are expected to be adaptively adjusted under different conditions. In this regard, the adaptive tuning method, proposed in [30], is utilized in this manuscript. This adaptive tuning approach is composed of two steps. In the first step, genetic algorithm (GA) is employed to determine the initial values of the coefficients under a driving cycle. In this work, GA is run by means of MATLAB. The twelve coefficients are defined as decision variables where GA tries to tune them in a way to minimize the defined cost function in (28). The obtained initial values of all the twelve weight coefficients are listed in Table IV. All the reported weight coefficients  $w_{opt,i}$  ( $i = 1, 2, 3$ ),  $w_{sgn,i}$  ( $i = 1, 2, 3$ ),  $w_{l,i}$  ( $i = 1, 2, 3$ ),  $w_{soc}$ ,  $w_{Bat,avg}$ ,  $w_{Bat,l}$  are then adaptively adjusted as follows, taking  $w_{opt,i}$  as an example:

$$if \quad |P_{FCi} - P_{FC_{opt},i}| \geq \varepsilon_{opt,i} \quad then \quad (i = 1, 2, 3)$$

$$w_{opt,i} : max[\min(w_{opt,i,max}, w_{opt,i}) + \Delta w_{opt,i}, w_{opt,i,min}]$$

$$if \quad |P_{FCi} - P_{FC_{opt},i}| < \varepsilon_{opt,i} \quad then$$

$$w_{opt,i} : max[\min(w_{opt,i,max}, w_{opt,i}) - \Delta w_{opt,i}, w_{opt,i,min}]$$

where  $\varepsilon_{opt,i}$  stands for the threshold value,  $w_{opt,i,max}$  and  $w_{opt,i,min}$  are the upper bound and lower bound, respectively, and  $\Delta w_{opt,i}$  is the tuning step size. All the parameters for the tuning of the weight coefficients are listed in Table IV.

$$P_{FC1} = \frac{S1 + w_{l,1} * a_1(P_{FC_{l,1}}) + w_{opt,1} * d_1(P_{FC_{opt,1}}) + w_{sgn,1} * P_{FC_{sgn,1}}}{G} \quad (23)$$

$$P_{Bat} = \frac{S2 + w_{Bat,avg} * f(P_{Bat,avg}) + w_{Bat,l} * c(P_{Bat,l}) + w_{soc} * g(P_{Bat,soc})}{G} \quad (24)$$

TABLE IV  
COEFFICIENT WEIGHT

Initial Value	Adaptive	Tuning
$w_{l,i} = 0.2$	$w_{l,i,max} = 1$	$w_{l,i,min} = 0.1$
$w_{opt,i} = 0.5$	$\Delta w_{l,i} = 0.001$	$\Delta w_{opt,i} = 0.001$
	$w_{opt,i,max} = 1$	$w_{opt,i,min} = 0.1$
	$w_{sgn,i,max} = 1$	$w_{sgn,i,min} = 0.1$
$w_{sgn,i} = 0.5$	$\Delta w_{sgn,i} = 0.001$	$w_{bat,l,max} = 1$
$w_{soc} = 0.2$	$w_{soc,max} = 1$	$w_{soc,min} = 0.1$
	$\Delta w_{soc} = 0.001$	$w_{bat,l,min} = 0.1$
$w_{bat,avg} = 0.2$	$w_{bat,avg,max} = 1$	$w_{bat,avg,min} = 0.1$
$w_{bat,l} = 0.2$	$\Delta w_{bat,avg} = 0.001$	$\Delta w_{bat,avg} = 0.001$

### B. Dynamic Programming

DP is a global optimization method that is used to solve an energy management problem in which the driving cycle is known in advanced. In this work, a multi-variable DP is required because there are multiple power sources. Such a tool has been already developed and successfully tested in solving the energy management optimization problem of various HEVs [30]. The provided MATLAB function in [30] is used in this study to solve the discrete-time optimal-control problem with DP algorithm. The utilized DP here minimizes the introduced cost function in (28). The considered system states are battery SOC and the power of each PEMFC system to avoid abrupt changes in the drawn power from the FCs. The considered dynamic constraints are as 10% of the MP per second for rising up, and 30% of the MP per second for falling down [31]. The steady space model is defined as:

$$x_{k+1} = \begin{cases} f(x_k, u_k, v_k, a_k) + x_k \\ x = [SOC, P_{FC1,SV}, P_{FC2,SV}, P_{FC3,SV}] \\ u = [P_{FC1,CV}, P_{FC2,CV}, P_{FC3,CV}, P_{Bat}] \end{cases} \quad (25)$$

where  $x_k$  is the vector of state variables,  $u_k$  is the vector of control variables,  $v_k$  is the vehicle velocity,  $a_k$  is the vehicle acceleration,  $i_k$  is the gear number,  $P_{FCi,SV}$  ( $i=1,2,3$ ) is the PEMFC power as a state variable,  $P_{FCj,CV}$  ( $j=1,2,3$ ) is the stack power as a control variable, and  $P_{Bat}$  is the battery power. Since the driving profile is a priori known,  $v_k$ ,  $a_k$ , and  $i_k$  can be incorporated in the model function. Consequently, the steady space model will be,

$$x_{k+1} = f(x_k, u_k, v_k) + x_x, k = 0, 1, \dots, N-1 \quad (26)$$

$$N = \frac{T_F}{T_s} + 1$$

where  $T_F$  is the final time of the driving cycle and  $T_s$  is the sampling time. The considered limitations on the control and state variables are defined as:

$$SOC_{min} \leq SOC \leq SOC_{max} \quad (27)$$

$$P_{Bat,min} \leq P_{Bat} \leq P_{Bat,max}$$

$$P_{FC,SV,min} \leq P_{FC,SV} \leq P_{FC,SV,max}$$

$$\Delta P_{FC,SV,rate,min} \leq \Delta P_{FC,SV,rate} \leq \Delta P_{FC,SV,rate,max}$$

$$\Delta P_{Bat,rate,min} \leq \Delta P_{Bat,rate} \leq \Delta P_{Bat,rate,max}$$

$$P_{FC,min} \leq P_{FCj,CV}(k) \leq P_{FC,max}$$

$$\begin{cases} SOC \in [50\%, 90\%] \\ P_{FCj,CV} \in [0, 7330 \text{ W}] \\ P_{FCi,SV} \in [0, 7330 \text{ W}] \\ \Delta P_{Bat,rate,min} \in [-36000, 36000 \text{ W s}^{-1}] \\ \Delta P_{FC,SV,rate,min} \in [-5000, 6600 \text{ W s}^{-1}] \end{cases}$$

where  $\Delta P_{FC,rate}$  and  $\Delta P_{Bat,rate}$  are the change rate of the FC and battery power respectively, the value of  $P_{FCi,SV}$  is considered based on [30]. Various minimum and maximum SOC levels for the battery have been considered in the literature [32]. In this work, a conservative level of 50% is considered for the minimum battery SOC. This choice provides a reasonable balance between charge and discharge efficiency [33]. The maximum SOC level is set to 90%. Lithium-ion batteries normally have a big flat low-resistance area in the middle. Therefore, the considered range for the battery SOC will be almost within this flat low-resistance area.

### C. Adaptive State Machine

An ASM based EMS is developed to be compared with the proposed GT strategy. This strategy has been introduced in [33] for a multi-stack FC-HEV. This strategy involves two steps. In the first step, RLS is responsible for determining MP and maximum efficiency of FCs and in the second step, some rules are utilized for performing the power split among power sources. In this strategy, FCs work on maximum efficiency until battery SOC level approaches the defined limits. If SOC is more than 90%, FCs turn off and if SOC is less than 50% FCs should work on the MP. FCs with less degradation supply more portion of the requested power. Moreover, to decrease the number of switching, FCs maintain their operation until the battery SOC constraint is satisfied.

### D. Evaluation Procedure

In order to evaluate the performance of the above-discussed strategies, the following cost function is employed. This implies that the discussed strategies are run for a driving cycle and then their performance will be quantified by (28) which

includes the hydrogen consumption and degradation in the FCs and the battery pack.

$$\$_{Total} = \left( \sum_{i=1}^3 \$_{FCi} \right) + \$_{H_2} + \$_{bat} \quad (28)$$

$$Deg_{FCi}(t) = \int_0^t \left( \frac{\delta_0}{3600} \left( 1 + \frac{\gamma}{P_{FC,nom}^2} (P_{FCi} - P_{FC,nom}^2) \right) + N_{switch} \eta_{switch} \right) dt$$

$$\$_{FCi} = Deg_{FCi}(t) FC_{cost} \quad (29)$$

$$\$_{H_2} = H_{2cost} \int_0^{\tau} \dot{m}_{H_2} dk \quad (30)$$

$$Deg_{bat}(t) = \frac{1}{Q_{bat}} \int_0^t |(1 + 3.25(1 - SOC)^2 i_{bat} G(i_{bat}))| dt \quad (31)$$

$$\begin{cases} G(i_{bat}) = 1 + 0.45 \frac{i_{bat}}{i_{bat-nom}} & \text{if } i_{bat} \geq 0 \\ G(i_{bat}) = 1 + 0.55 \frac{|i_{bat}|}{i_{bat-nom}} & \text{if } i_{bat} < 0 \end{cases} \quad (32)$$

$$\$_{bat} = Bat_{cost} Deg_{bat}(t) \quad (33)$$

Where  $\$_{FC}$  is FC degradation cost,  $\$_{H_2}$  is the cost of fuel consumption,  $\$_{bat}$  is the battery system degradation cost,  $Deg_{FC}$  is the degradation of FC,  $FC_{cost}$  is the FC system cost that is 600 US\$,  $N_{switch}$  is the number of start-stop of the FC,  $\eta_{switch}$  is the start-stop degradation coefficient [34],  $\delta_0$  and  $\alpha$  are load coefficients,  $P_{FC,nom}$  is the nominal power of the FC in terms of degradation,  $H_{2cost}$  is the cost of hydrogen consumption that is 3.5 US \$/kgH<sub>2</sub>,  $Deg_{bat}$  is the degradation of battery,  $Bat_{cost}$  is the cost of degradation of battery that is 640 US\$,  $Q_{bat}$  is the capacity of battery,  $i_{bat-nom}$  is the nominal current of battery and  $i$  is the number of FC.

#### IV. RESULTS AND DISCUSSION

To comprehensively evaluate the performance of the proposed EMS, two case studies have been designed under a real driving cycle, as explained hereinafter. Fig. 7 presents the utilized real driving cycle in this study and its respective requested power that should be supplied by the power sources. This driving cycle has been obtained by an on-road test drive of the real studied three-wheel motorcycle (Spyder) [20], [35]. It has been designed based on the characteristics of this recreational three-wheel motorcycle which normally experiences high accelerations and decelerations. The employed driving cycle comprises an urban driving condition with two rapid accelerations (0 to 70 km/h in 8 s) and two fast decelerations in order to challenge this reactional vehicle. The maximum speed is about 90 km/h and the overall driven distance throughout this test is 30 km.

Firstly, the performance of the proposed online EMS based on GT is compared with DP, as an offline optimal strategy, and ASM, that is a competent rule-based strategy. This first case study clarifies the potential of the GT as an online EMS in such a multi-source system by measuring how far its results are compared to an ideal case (comparison with DP) and how

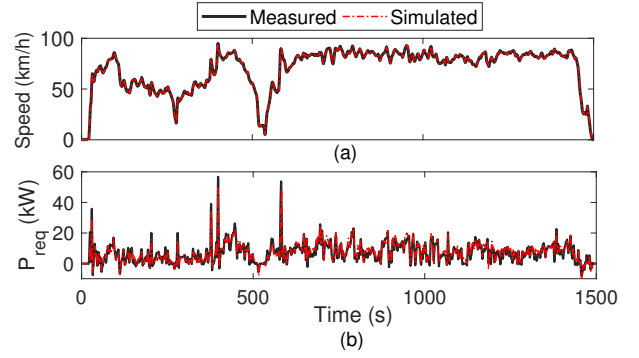


Fig. 7. Real driving cycle e-TESC: (a) Speed, (b) Corresponding requested power.

it performs compared to another available online EMS used for multi-stack FC-HEVs in the literature. Fig. 8 shows the distribution of the power among the three FCs and the variation of battery SOC after imposing the real driving profile to the vehicle. Fig. 8(a) shows the power distribution by GT in which it is evident that each FC, as a player, tries to maximize its utility function. Since all the FCs have the same degradation level, the requested power from them follows the same trend. Fig. 8(b) illustrates the power distribution by ASM strategy where the FCs are turned on in a specific order to supply the requested power. Looking at the performance of ASM strategy, it is observed that some FC on/off cycles happen during the power distribution by this strategy as it tries to use the minimum number of FCs. However, the on/off cycles are very limited in case of GT. Fig. 8(c) presents the power split performed by DP where all the three FCs show the same behavior since the strategy is aware of the driving cycle in advance. Fig. 7(d) demonstrates the variation of battery SOC for each of the discussed EMSs. It should be noted that all the strategies start with the same initial SOC. To have a fair comparison, first, GT-based EMS performs the power distribution and results in a particular final SOC (61%). Afterwards, the final battery SOC for DP is set to reach the same value as GT. The final battery SOC for ASM strategy is a bit lower than other strategies. This difference affects the hydrogen consumption comparison. Therefore, a recharge step at the end of each profile is considered for ASM strategy. In this regard, the battery is recharged to reach the same final SOC as other strategies by using the maximum efficiency point of the PEMFC stack at the end of each test and the US\$ cost of the additional required hydrogen is added to the total cost function. To better comprehend the behavior of the FCs while being used by the strategies to supply the requested power, the distribution of power for different cases is presented in form of histogram in Fig. 9. According to this figure, the density of power points is high within the efficient zone of the FCs (around 2 kW) in both of GT and DP strategies under the Real driving cycle e-TESC. Moreover, the FCs have almost the same distribution pattern in GT which is a solid proof that the defined utility functions try their best to maximize their preferences. Regarding the ASM strategy, the distribution patterns of FCs are different with one another at each driving

cycle since the main policy of this strategy is to supply the requested power by using the minimum number of FCs.

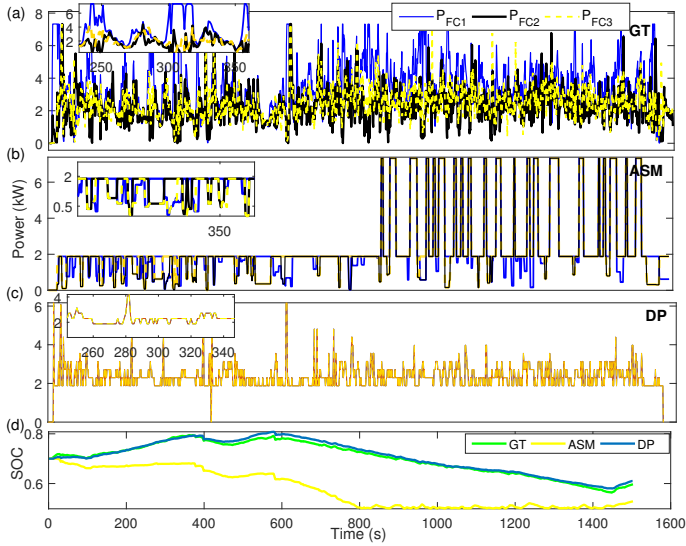


Fig. 8. The allocation of power among FCs under real driving cycle e-TESSC: (a) GT, (b) ASM, (c) DP, (d) Battery SOC.

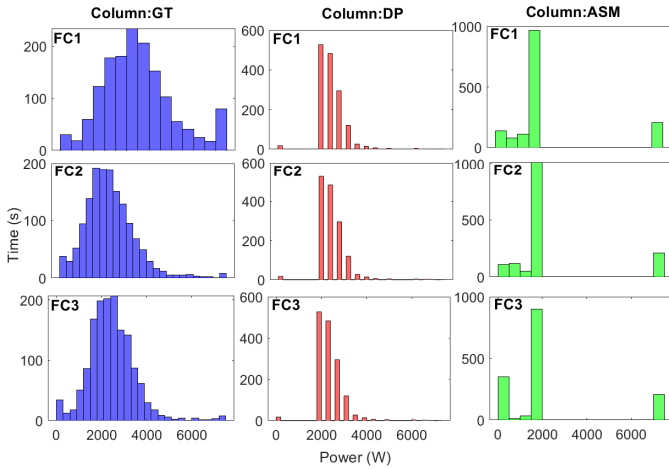


Fig. 9. Distribution of the FCs power points for the three strategies under real driving cycle e-TESSC.

Table V summarizes the results of the discussed comparative study regarding the three EMSs in terms of different performance indexes. From this table, DP has reached the minimum total cost (0.6 USD), followed by GT (0.68 USD) and ASM (0.723 USD). This implies that GT has achieved the nearest total cost to DP by almost 12% difference while the total cost difference between ASM and DP is around 18%. Comparison of hydrogen consumption shows that, ASM has consumed less hydrogen than GT to accomplish the power allocation. This is mainly due to the fact ASM uses the minimum number of FCs to supply the power. However, looking at the degradation costs of FCs and battery illustrate that the policy of ASM for minimizing the hydrogen consumption has led to the increase of the degradation costs compared to GT.

In the second case study, the impact of power sources' degradation on the performance of the proposed EMS is

TABLE V  
COMPARISON OF DIFFERENT EMSs

Performance index	EMS		
	GT	DP	ASM
Total cost (US\$)	0.68	0.6	0.723
On/Off cycles	FC1=0 FC2=0 FC3=0	FC1=1 FC2=1 FC3=1	FC1=0 FC2=0 FC3=0
H2 consumption (g)	184	153	181
Battery degradation cost (US\$)	0.0032	0.0022	0.0457
FC degradation cost (US\$)	0.0376	0.05	0.0376

investigated. This is to show the necessity of updating the parameters of the FCs and battery online to prevent the strategy from malfunction. In this case study, only GT-based EMS is utilized for distributing the power among the sources in three different situations. In the first situation, called  $GT_{new}$ , all the power sources are healthy, and no degradation has happened. Therefore, the parameters setting of the strategy is based on healthy power sources. In the second situation, called  $GT_{Degraded}$ , it is assumed that all the power sources have become degraded, and the parameters setting is also adapted to the degraded health state of the power sources. It should be noted that a 10-percent decline in the MP of the FCs and twofold increase in internal resistance of the battery pack have been considered in the simulation to have degraded power sources. In the third situation, called false input feedback  $GT_{Nofeedback}$ , it is assumed that the power sources have become degraded but the parameters setting of the strategy has not been updated. This is exactly the case that can happen in an EMS which is not equipped with an online identification process to update the parameters setting. The comparison of the first and second situations clarifies the influence of the power sources' degradation over the performance of the EMS when it is aware of the occurred attenuation. However, the third situation highlights the importance of updating the parameters setting when performance attenuation occurs in the power sources which is the responsibility of the developed online identification process in this study. Fig. 10 shows the battery SOC variation of three explained situations under the real driving profile. The SOC of  $GT_{new}$  has achieved the highest final level compared to other two situations particularly in Fig. 10. This difference of final battery SOC can highly influence the hydrogen consumption as presented in Fig. 10. From Fig. 11, it is observed that when the power sources have become degraded and the EMS is aware of this uncertainty, the hydrogen consumption increases by 32% for real driving profile. However, when the power sources degrade and the EMS is unaware of it, the hydrogen consumption increases by almost 39%. These results confirm that integrating the online updating strategies into the EMS design is a key step towards minimizing the hydrogen consumption.

## V. CONCLUSION

This paper puts forward a GT-based EMS to distribute the power among three FCs and a battery pack. The de-

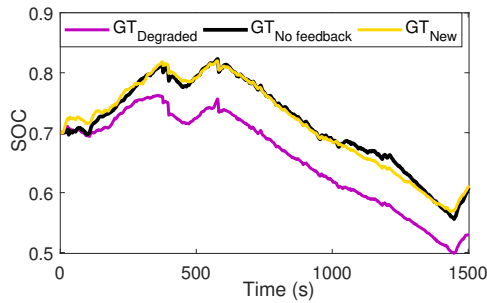


Fig. 10. Battery SOC variation for Real driving cycle e-TESS.

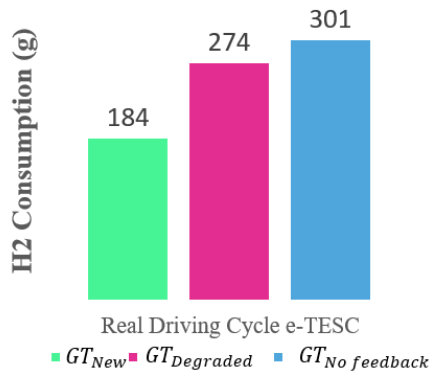


Fig. 11. Hydrogen consumption comparison of different scenarios.

defined functions are used to control the on/off cycles in the FC, minimize the hydrogen consumption and degradation of the power sources. Furthermore, an online parameter identification method is used for each power source to update the utilized parameters, such as MP, battery SOC, etc., in the EMS. To evaluate the performance of the proposed strategy, it is compared with DP and an ASM based method under the real driving cycle. The obtained total cost of hydrogen consumption and degradation of the developed GT strategy is around 6% less than the ASM and 12% higher than DP. The last analysis of this manuscript deals with investigating the impact of degradation of the power sources on the hydrogen consumption of the utilized multi-stack FC-HEV architecture. The results demonstrates that when the EMS is not aware of the health state of the power sources, the hydrogen consumption can rise up to 7% in the studied system. Although this manuscript has pointed out the potential of the suggested EMS, some prospects for expanding the scope of this work remain as follows:

- Adding a braking strategy to the developed powertrain configuration of this manuscript to enhance the overall efficiency of the studied FC-HEV. In fact, in the utilized three-wheel motorcycle, there is only one electric motor connected to the rear wheels and to avoid the skid of the rear wheel, regenerative capacity should be limited. So, further study should be done to safely add full regenerative braking for this specific design.
- Designing a specific scheme for prioritizing the activation and deactivation of individual FC stacks.

## REFERENCES

- [1] M. Kandidayeni, A. O. M. Fernandez, A. Khalatbarisoltani, L. Boulon, S. Kelouwani, and H. Chaoui, "An online energy management strategy for a fuel cell/battery vehicle considering the driving pattern and performance drift impacts," *IEEE Transactions on Vehicular Technology*, vol. 68, no. 12, pp. 11 427–11 438, 2019.
- [2] D. Fares, R. Chedid, F. Panik, S. Karaki, and R. Jabr, "Dynamic programming technique for optimizing fuel cell hybrid vehicles," *International Journal of Hydrogen Energy*, vol. 40, no. 24, pp. 7777–7790, 2015.
- [3] T. Zeng, C. Zhang, Y. Zhang, C. Deng, D. Hao, Z. Zhu, H. Ran, and D. Cao, "Optimization-oriented adaptive equivalent consumption minimization strategy based on short-term demand power prediction for fuel cell hybrid vehicle," *Energy*, vol. 227, p. 120305, 2021.
- [4] K. Song, X. Wang, F. Li, M. Sorrentino, and B. Zheng, "Pontryagin's minimum principle-based real-time energy management strategy for fuel cell hybrid electric vehicle considering both fuel economy and power source durability," *Energy*, vol. 205, p. 118064, 2020.
- [5] B. Geng, J. K. Mills, and D. Sun, "Two-stage energy management control of fuel cell plug-in hybrid electric vehicles considering fuel cell longevity," *IEEE Transactions on vehicular technology*, vol. 61, no. 2, pp. 498–508, 2011.
- [6] S. Caux, W. Hankache, M. Fadel, and D. Hissel, "On-line fuzzy energy management for hybrid fuel cell systems," *International journal of hydrogen energy*, vol. 35, no. 5, pp. 2134–2143, 2010.
- [7] A. Serpi and M. Porru, "An mpc-based energy management system for a hybrid electric vehicle," in *2020 IEEE Vehicle Power and Propulsion Conference (VPPC)*. IEEE, 2020, pp. 1–6.
- [8] E. G. Amaya, H. G. Chiacchiarini, and C. De Angelo, "Energy management system designed for reducing operational costs of a hybrid fuel cell-battery-ultracapacitor vehicle," in *2020 IEEE Vehicle Power and Propulsion Conference (VPPC)*. IEEE, pp. 1–5.
- [9] C. Jia, W. Qiao, and L. Qu, "A cost-oriented control strategy for energy management of a dual-mode locomotive," in *2019 IEEE Vehicle Power and Propulsion Conference (VPPC)*. IEEE, 2019, pp. 1–6.
- [10] M. Ansarey, M. S. Panahi, H. Ziarati, and M. Mahjoob, "Optimal energy management in a dual-storage fuel-cell hybrid vehicle using multi-dimensional dynamic programming," *Journal of Power Sources*, vol. 250, pp. 359–371, 2014.
- [11] N. Marx, L. Boulon, F. Gustin, D. Hissel, and K. Agbossou, "A review of multi-stack and modular fuel cell systems: Interests, application areas and on-going research activities," *International Journal of Hydrogen Energy*, vol. 39, no. 23, pp. 12 101–12 111, 2014.
- [12] B. Somaiah and V. Agarwal, "Distributed maximum power extraction from fuel cell stack arrays using dedicated power converters in series and parallel configuration," *IEEE Transactions on Energy Conversion*, vol. 31, no. 4, pp. 1442–1451, 2016.
- [13] N. Marx, D. Hissel, F. Gustin, L. Boulon, and K. Agbossou, "On the sizing and energy management of an hybrid multi-stack fuel cell-battery system," in *International Conference on Renewable Energy: Generation and Applications*, 2016.
- [14] Y. Yan, Q. Li, W. Chen, W. Huang, and J. Liu, "Hierarchical management control based on equivalent fitting circle and equivalent energy consumption method for multiple fuel cells hybrid power system," *IEEE Transactions on Industrial Electronics*, vol. 67, no. 4, pp. 2786–2797, 2019.
- [15] T. Wang, Q. Li, H. Yang, L. Yin, X. Wang, Y. Qiu, and W. Chen, "Adaptive current distribution method for parallel-connected pemfc generation system considering performance consistency," *Energy Conversion and Management*, vol. 196, pp. 866–877, 2019.
- [16] A. Khalatbarisoltani, M. Kandidayeni, L. Boulon, and X. Hu, "Power allocation strategy based on decentralized convex optimization in modular fuel cell systems for vehicular applications," *IEEE Transactions on Vehicular Technology*, 2020.
- [17] Z. Sun, Y. Wang, Z. Chen, and X. Li, "Min-max game based energy management strategy for fuel cell/supercapacitor hybrid electric vehicles," *Applied Energy*, vol. 267, p. 115086, 2020.
- [18] Q. Zhang, J. Han, G. Li, and Y. Liu, "An adaptive energy management strategy for fuel cell/battery/supercapacitor hybrid energy storage systems of electric vehicles," *International Journal of Electrochemical Science*, vol. 15, no. 4, pp. 3410–3433, 2020.
- [19] R. Ghaderi, M. Kandidayeni, M. Soleymani, L. Boulon, and H. Chaoui, "Online energy management of a hybrid fuel cell vehicle considering the performance variation of the power sources," *IET Electrical Systems in Transportation*, vol. 10, no. 4, pp. 360–368, 2020.

- [20] J. P. F. Trovão, M.-A. Roux, É. Ménard, and M. R. Dubois, "Energy-and power-split management of dual energy storage system for a three-wheel electric vehicle," *IEEE Transactions on Vehicular Technology*, vol. 66, no. 7, pp. 5540–5550, 2016.
- [21] C. Dépature, W. Lhomme, P. Sicard, A. Bouscayrol, and L. Boulon, "Real-time backstepping control for fuel cell vehicle using supercapacitors," *IEEE Transactions on Vehicular Technology*, vol. 67, no. 1, pp. 306–314, 2017.
- [22] G. Squadrito, G. Maggio, E. Passalacqua, F. Lufrano, and A. Patti, "An empirical equation for polymer electrolyte fuel cell (pefc) behaviour," *Journal of Applied Electrochemistry*, vol. 29, no. 12, pp. 1449–1455, 1999.
- [23] K. Ettahir, M. H. Cano, L. Boulon, and K. Agbossou, "Design of an adaptive ems for fuel cell vehicles," *International Journal of Hydrogen Energy*, vol. 42, no. 2, pp. 1481–1489, 2017.
- [24] H. Chen, P. Pei, and M. Song, "Lifetime prediction and the economic lifetime of proton exchange membrane fuel cells," *Applied Energy*, vol. 142, pp. 154–163, 2015.
- [25] X. Zhao, Y. Li, Z. Liu, Q. Li, and W. Chen, "Thermal management system modeling of a water-cooled proton exchange membrane fuel cell," *International Journal of Hydrogen Energy*, vol. 40, no. 7, pp. 3048–3056, 2015.
- [26] H. F. Gharibeh, A. S. Yazdankhah, and M. R. Azizian, "Energy management of fuel cell electric vehicles based on working condition identification of energy storage systems, vehicle driving performance, and dynamic power factor," *Journal of Energy Storage*, vol. 31, p. 101760, 2020.
- [27] P. Shen, M. Ouyang, L. Lu, J. Li, and X. Feng, "The co-estimation of state of charge, state of health, and state of function for lithium-ion batteries in electric vehicles," *IEEE Transactions on vehicular technology*, vol. 67, no. 1, pp. 92–103, 2017.
- [28] M. Kandidayeni, A. Macias, A. Amamou, L. Boulon, S. Kelouani, and H. Chaoui, "Overview and benchmark analysis of fuel cell parameters estimation for energy management purposes," *Journal of power sources*, vol. 380, pp. 92–104, 2018.
- [29] X. Hu, C. Zou, X. Tang, T. Liu, and L. Hu, "Cost-optimal energy management of hybrid electric vehicles using fuel cell/battery health-aware predictive control," *IEEE Transactions on Power Electronics*, vol. 35, no. 1, pp. 382–392, 2019.
- [30] W. Zhou, L. Yang, Y. Cai, and T. Ying, "Dynamic programming for new energy vehicles based on their work modes part ii: Fuel cell electric vehicles," *Journal of Power Sources*, vol. 407, pp. 92–104, 2018.
- [31] M. Carignano, V. Roda, R. Costa-Castelló, L. Valiño, A. Lozano, and F. Barreras, "Assessment of energy management in a fuel cell/battery hybrid vehicle," *IEEE access*, vol. 7, pp. 16 110–16 122, 2019.
- [32] N. Sulaiman, M. Hannan, A. Mohamed, E. Majlan, and W. W. Daud, "A review on energy management system for fuel cell hybrid electric vehicle: Issues and challenges," *Renewable and Sustainable Energy Reviews*, vol. 52, pp. 802–814, 2015.
- [33] A. M. Fernandez, M. Kandidayeni, L. Boulon, and H. Chaoui, "An adaptive state machine based energy management strategy for a multi-stack fuel cell hybrid electric vehicle," *IEEE Transactions on Vehicular Technology*, vol. 69, no. 1, pp. 220–234, 2019.
- [34] C. Depature, S. Jemei, L. Boulon, A. Bouscayrol, N. Marx, S. Morando, and A. Castaings, "Ieee vts motor vehicles challenge 2017-energy management of a fuel cell/battery vehicle," in *2016 IEEE Vehicle Power and Propulsion Conference (VPPC)*, 2016, pp. 1–6.
- [35] A. Macias, M. Kandidayeni, L. Boulon, and J. Trovão, "Fuel cell-supercapacitor topologies benchmark for a three-wheel electric vehicle powertrain," *Energy*, vol. 224, p. 120234, 2021.



**Razieh Ghaderi** (Razieh.Ghaderi@uqtr.ca) received the B.S. degree in telecommunication engineering in 2017, the master's degree in mechatronics from Arak University, Iran, in 2020. She is currently working towards the Ph.D. degree in electrical engineering at Université du Québec à Trois-Rivières, QC, Canada. Her research interests include the development of energy management strategies for hybrid systems, fuel cell and battery modeling.



**Mohsen Kandidayeni** (Member, IEEE) received his Ph.D. degree (Hons.) in electrical engineering from University of Quebec in Trois-Rivières (UQTR), QC, Canada, in 2020. He is currently a post-doctoral researcher at e-TESC lab in University of Sherbrooke, and a research assistant in the Hydrogen Research Institute of UQTR. He has been actively involved in conducting research through authoring, coauthoring, and reviewing several articles in different prestigious scientific journals. His research interest includes energy related topics, such as hybrid electric vehicles, fuel cell systems, energy management, and control. Moreover, he has been the recipient of several awards/honors during his educational path, such as the doctoral and post-doctoral Scholarships from FRQNT.



**Mehdi Soleymani** received his BSc, MSc, and PhD degrees from Iran University of Science and Technology (IUST) in 2000, 2003, and 2009 respectively. He has been with Arak University as an associate professor of mechanical engineering from 2015 up to the present. He was with the Advanced Vehicle Engineering Centre (AVEC) at Cranfield University as a research fellow from 2018 to 2021. Currently he is with the hydrogen research institute of UQTR as an invited professor. His research interest includes active vibration control in vehicles and structural systems and energy storage and energy management systems for hybrid electric, fuel cell, and electric vehicles.



**Loïc Boulon** is a professor at UQTR (Full Professor since 2016) and he works into the Hydrogen Research Institute (Deputy director since 2019). His work deals with modeling, control and energy management of multiphysics systems. His research interests include hybrid electric vehicles, energy and power sources (fuel cell systems, batteries and ultracapacitors). He has published more than 140 scientific papers in peer-reviewed international journals and international conferences and given over 40 invited conferences all over the world. In 2019, he is the world most cited authors of the topic "Proton exchange membrane fuel cells (PEMFC); Fuel cells; Cell stack" in Elsevier SciVal. Prof. Loïc Boulon is VP-Motor Vehicles of the IEEE Vehicular Technology Society and he found the "IEEE VTS Motor Vehicle Challenge". He is now the Director of the Réseau Québécois sur l'Énergie Intelligente.



**João Pedro F. Trovão** (Joao.Trovao@USherbrooke.ca) (SM'17) received his Ph.D. degree in electrical engineering from the University of Coimbra, Portugal, in 2013. He is a professor with the Department of Electrical Engineering and Computer Engineering, University of Sherbrooke, Sherbrooke, QC, Canada, where he holds the Canadian Research Chair position in Efficient Electric Vehicles with Hybridized Energy Storage Systems. He is an author/coauthor of over 150 journal and conference papers. His research interests cover the areas of electric vehicles, hybridized energy storage systems, energy management and rotating electrical machines. Dr. Trovão was the General Chair of the 2018 IEEE Vehicle Power and Propulsion Conference, Chicago, US and He is a Senior Editor for the Automotive Electronics topic of the IEEE Vehicular Technology Magazine.